

## ORIGINAL ARTICLE

## Inhibitory control and error monitoring by human subthalamic neurons

J Bastin<sup>1,2</sup>, M Polosan<sup>1,2,3</sup>, D Benis<sup>1,2</sup>, L Goetz<sup>1,2</sup>, M Bhattacharjee<sup>1,2</sup>, B Piallat<sup>1,2</sup>, A Krainik<sup>2,4</sup>, T Bougerol<sup>3</sup>, S Chabardès<sup>1,2,5</sup> and O David<sup>1,2</sup>

The subthalamic nucleus (STN) has been shown to be implicated in the control of voluntary action, especially during tasks involving conflicting choice alternatives or rapid response suppression. However, the precise role of the STN during nonmotor functions remains controversial. First, we tested whether functionally distinct neuronal populations support different executive control functions (such as inhibitory control or error monitoring) even within a single subterritory of the STN. We used microelectrode recordings during deep brain stimulation surgery to study extracellular activity of the putative associative-limbic part of the STN while patients with severe obsessive-compulsive disorder performed a stop-signal task. Second, 2–4 days after the surgery, local field potential recordings of STN were used to test the hypothesis that STN oscillations may also reflect executive control signals. Extracellular recordings revealed three functionally distinct neuronal populations: the first one fired selectively before and during motor responses, the second one selectively increased their firing rate during successful inhibitory control, and the last one fired selectively during error monitoring. Furthermore, we found that beta band activity (15–35 Hz) rapidly increased during correct and incorrect behavioral stopping. Taken together, our results provide critical electrophysiological support for the hypothesized role of the STN in the integration of motor and cognitive-executive control functions.

*Translational Psychiatry* (2014) 4, e439; doi:10.1038/tp.2014.73; published online 9 September 2014

## INTRODUCTION

The ability to inhibit inappropriate responses (inhibitory control) or to monitor the consequences of actions (performance monitoring) corresponds to two forms of executive control functions involved in the planning and adaptation of goal-directed behavior in response to environmental or internal changes.<sup>1,2</sup> Executive control is impaired in patients with obsessive-compulsive disorder (OCD)<sup>3–5</sup> because compulsions and obsessions reflect a deficit of inhibitory control and abnormal action monitoring signals, respectively.<sup>3–6</sup> These executive impairments could be due to functional and anatomical abnormalities of cortico-basal ganglia-thalamocortical associative-limbic loops.<sup>3,4,7</sup>

The therapeutic effects of subthalamic nucleus (STN) high-frequency deep brain stimulation (DBS) in both motor (Parkinson's disease<sup>8</sup>) and nonmotor (OCD<sup>9–12</sup>) diseases strongly suggest that the STN is involved within the motor, cognitive and limbic cortico-basal ganglia-thalamocortical loops.<sup>7,13,14</sup> In addition, current neurocognitive models assume that the STN activity increases during action inhibition, response re-adjustments following conflicting situations,<sup>15–20</sup> facial emotion perception<sup>21</sup> or feedback-related motor learning.<sup>22</sup>

We reasoned that this variety of cognitive processes involving the human STN might be supported by functionally distinct but colocalized neuronal populations, within each of the motor, limbic and associative STN subterritories that have been shown to overlap in monkey.<sup>23</sup> To study the precise physiological mechanisms at the single-cell level that mediate inhibitory control and performance monitoring, we recorded neuronal activity of single and multiunits whereas OCD patients undergoing DBS surgery

performed a stop-signal task (SST). In addition, we recorded local field potentials (LFPs) to examine STN oscillatory modulations in the same patients performing the same task during the few days after the surgery.

The SST was used to experimentally dissociate motor action, stopping and error-monitoring signals.<sup>1,24,25</sup> It consisted of the random presentation of two trial types (Figure 1c). During GO trials (67% of trials), an imperative GO cue prompted patients to quickly press a button with the right index. During STOP trials (33% of trials), patients were asked to withhold the planned movement. To investigate the hypothesized 'braking function' of STN neurons during response selection, we contrasted successful stop trials (SS) with GO trials. To isolate error monitoring signals, unsuccessful stop (US) trials were compared with GO and SS trials.<sup>24–30</sup> Furthermore, behavioral responses during the SST allowed the estimation of the stop-signal reaction time (SSRT), which corresponds to the latency at which executive processes underlying successful motor inhibition terminate.<sup>1</sup> Thus, STN responses preceding the SSRT may encode stopping signals whereas STN responses occurring after the SSRT may be associated with performance monitoring signals.<sup>24,25,31</sup>

## MATERIALS AND METHODS

All patients provided their informed consent to participate to this study that was approved by our local ethical committee (Grenoble University Hospital, protocol number: 2011—A00083-38). Seven patients (3 males; mean age 37 ± 8.7 years old) undergoing bilateral surgical implantation of DBS electrodes in the STN to treat severe drug- and psychotherapy-resistant OCD were involved (Supplementary Table S1).<sup>9,10,12</sup> The Y-BOCS

<sup>1</sup>Fonctions Cérébrales et Neuromodulation, Université Joseph Fourier, Grenoble, France; <sup>2</sup>Grenoble Institut des Neurosciences, INSERM, U836, Grenoble, France; <sup>3</sup>Clinique de Psychiatrie, Pôle Neurologie Psychiatrie, Centre Hospitalier Universitaire, Grenoble, France; <sup>4</sup>Clinique de Neuroradiologie, Pôle Imagerie, Centre Hospitalier Universitaire, Grenoble, France and <sup>5</sup>Clinique de Neurochirurgie, Pôle Tête et Cou, Centre Hospitalier Universitaire, Grenoble, France. Correspondence: Dr J Bastin, Institut des Neurosciences de Grenoble, Bâtiment Edmond J. Safra des Neurosciences, Chemin Fortuné Ferrini, Université Joseph Fourier, Site Santé La Tronche, BP 170, 38042 Grenoble Cedex 9, France.

E-mail: julien.bastin@ujf-grenoble.fr

Received 27 August 2013; revised 30 June 2014; accepted 14 July 2014

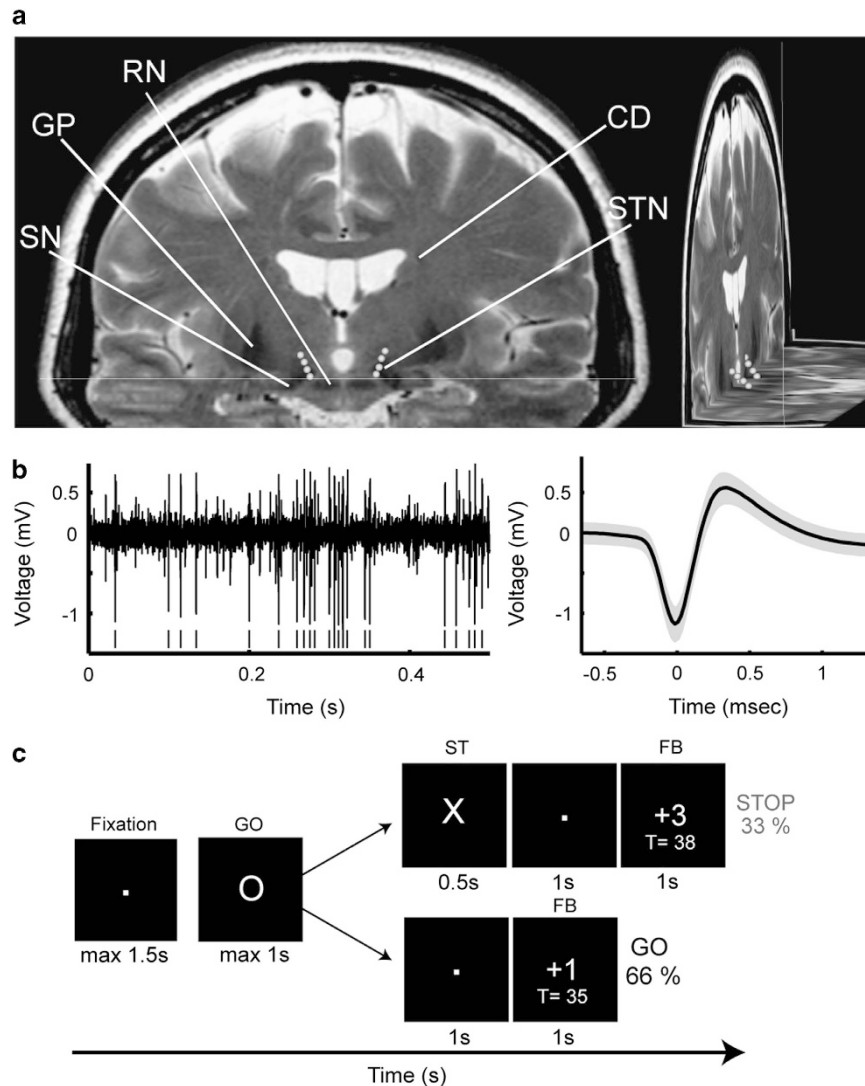


**Figure 1.** (a) Localization of DBS electrodes contacts on axial and coronal MRI sections of a patient. (b) Microelectrode STN recording and mean waveform (black)  $\pm$  s.d. (gray) of the isolated spike cluster. (c) Stop-signal task. Participants were instructed to respond as fast as they can to the GO cue and to withhold their response when a stop signal occurs. Task difficulty during STOP trials was adjusted by shortening or lengthening the delay between GO and STOP cues (stop-signal delay, SSD) after unsuccessful or successful STOP trials. After each trial, positive and negative feedback was presented for 1 s (see Materials and Methods). CD, caudate nucleus; DBS, deep brain stimulation; GP, globus pallidus; MRI, magnetic resonance imaging; RN, red nucleus; SN, substantia nigra; STN, subthalamic nucleus.

score was  $33.8 \pm 0.6$ , on a scale from 0–40, with lower scores indicating less severe symptoms. Patients were off medications during the surgery (12-h washout) whereas they were on medication during the postoperative experiment (see Supplementary Table S1).

Patients completed 100 SST trials during each intraoperative SST experiment. On average, a patient could complete  $5.3 \pm 0.7$  experiments (between two and three experiments for each side of implantation). During the postoperative recording experiment, patients completed eight experiments of the same protocol (800 SST trials per patient). During the SST, two types of trials were presented in a randomized order (Figure 1). In GO trials (66% of trials), an imperative GO cue prompted patients to quickly press a button with the right index after a variable fixation period (the range was 800–1200 ms). GO cue vanished after button press or after 1000 ms. In STOP trials (33% of trials), a STOP signal unpredictably followed the imperative GO cue after a variable stop-signal delay (SSD). Trial order was randomized. STOP cue vanished after 500 ms or after button press. The ability to stop a response is related to SSD value: the longer the SSD, the more difficult it is to stop.<sup>1</sup> The SSD was thus varied from trial to trial to adjust task difficulty using a procedure composed of a single staircase to obtain successful withholding of button press in approximately 50% of

STOP trials (50 ms steps). The initial SSD was set to 200 ms and the range varied from one patient to another (across patients, we observed extreme SSD values ranging from 16–800 ms). This procedure provided a simple estimation of patients' time needed to cancel the movement (SSRT), which can be estimated from a simple race model between the motor and inhibitory processes.<sup>1</sup> The SSRT was computed using the integration method.<sup>32</sup> To maintain high attentional and motivational level despite the repetitive nature of the SST, a feedback appeared during 1500 and 1000 ms after GO or STOP trials to indicate success or failure. Successful GO or STOP trials were accompanied by a score increase of 1 or 3 points, respectively, whereas failed trial feedback consisted of losing 1 or 3 points, respectively. Button presses had to occur before 1000 ms after GO cue to be considered as successful. During feedback, both score increase/decrease in the current trial and the total number of points obtained during the session were displayed. Visual stimuli were delivered on a 15.4-inch monitor with a refresh rate of 60 Hz with Presentation 14.1 (Neurobehavioral Systems, Albany, CA, USA). Patients responded to the task through right index finger button presses.

As in routine DBS procedure of Grenoble University Hospital, five tungsten microelectrodes (2 mm apart, tip diameter  $< 10 \mu\text{m}$ ; impedance

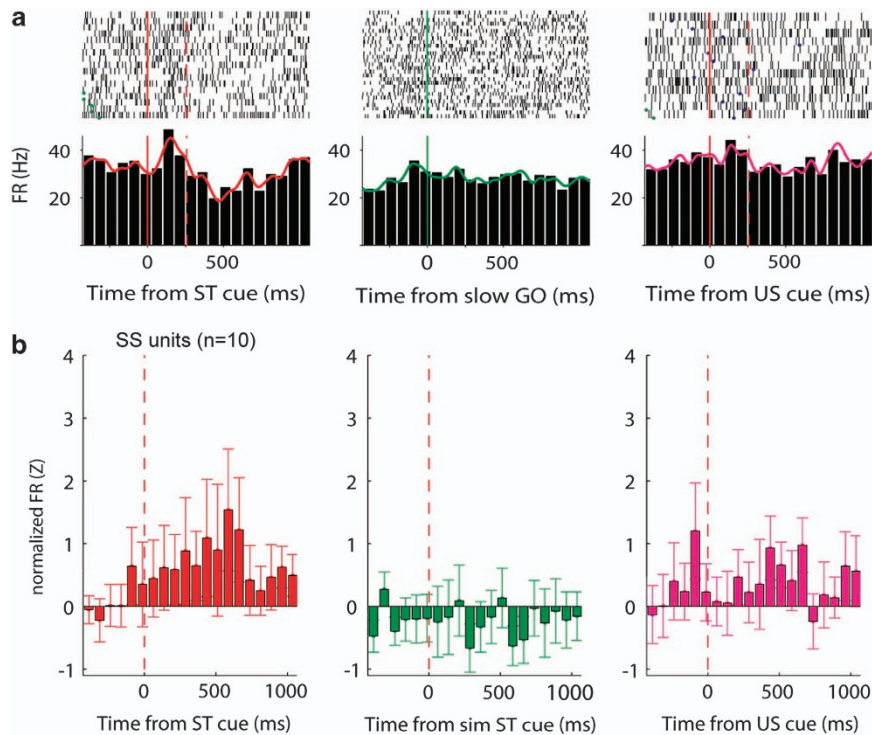


**Figure 2.** Selective response of STN neurons during stopping, shown as rastergrams (black dots), SDF (continuous lines) and PSTH across trial types (SS, US, LMGO). **(a)** Representative SS unit. In rastergrams, green dots indicate the onset of GO cue and blue dots indicate the time of incorrect button press. Trials are sorted according to their stop-signal delay (SS and US trials) or motor reaction time (GO trials). Time origin indicates stop cue during SS and US trials and simulated stop cue during LMGO trials. Vertical dashed red line indicates SSRT during this SST experiment. **(b)** Normalized population activity of all recorded SS units ( $n = 10$ ). Error bars indicate s.e.m. LMGO, latency-matched GO; PSTH, peri-stimulus spike histogram; SDF, spike density function; SS, successful stop trial; SSRT, stop-signal reaction time; SST, stop-signal task; STN, subthalamic nucleus; US, unsuccessful stop trial.

of 0.2–6 M $\Omega$  at 1 KHz, FHC microelectrodes, Bowdoinham, ME, USA) were used to optimize STN targeting based on the spiking properties of STN cells (Figures 1a and b, see Supplementary Text and Supplementary Figure S1 for more information on STN localization). Raw neuronal activity was amplified ( $\times 10$ ), band-pass filtered between 300 and 6000 Hz and sampled at 48 kHz. The STN was preoperatively targeted using stereotactic magnetic resonance imaging and the OCD target was defined 2 mm anterior and 1 mm medial to the Parkinson's disease target, at the presumed boundary of nonmotor and motor STN.<sup>12</sup> Spike detection and spike sorting was applied to continuous data using Waveclus clustering algorithm.<sup>33</sup> Subsequently, clusters were classified into single or multiunits according to a criterion based on the spike shape and variance, the signal-to-noise ratio and the refractory period observed in the inter-spike interval histograms.<sup>34</sup>

To quantify each identified cluster spike activity during the task, peri-stimulus spike histograms (100 ms bins; 2000 ms time window centered on the event) and continuous neuronal activation function (spike density functions, SDFs) were generated. SDFs were obtained by convolving each spike with a Gaussian kernel (s.d. = 100 ms). To statistically estimate whether each neuronal unit significantly responded to the task, we used a bootstrap randomization process (resampling test) that was applied 1000 times by shuffling the spike timing within each trial type (SS, US, GO). The resampling method maintained the number of observed spikes and the inter-spike interval distribution during each trial and allowed computing a surrogate peri-stimulus spike histogram. This procedure tests the null hypothesis that spikes are randomly distributed across time around the task event. Hence, if spiking activity from the original peri-stimulus spike histogram fell outside the 95% confidence interval of the permuted set, the activity was declared to be significantly modulated by the task event.

Task-responsive neurons were classified in three functional clusters according to the following criteria. SS units preferentially responded during SS trials. SS units had to display a firing rate in a 1000-ms window after the stop cue that was superior to the firing rate observed during the 50% slower proportion of GO trials (latency-matched GO, LMGO) and to the firing rate observed during US trials. Neuronal activity was aligned to

stop cues during SS and US whereas it was aligned to a virtual stop during LMGO trials. The virtual stop was introduced during LMGO using the distribution of SSD observed during SS trials so that going (LMGO trials) and stopping (SS) processes could be directly compared. This procedure was preferred to the alternative possibility to align neural activity on GO cues because preliminary analyses showed that this procedure suppressed neural responses observed during SS trials, reflecting the variability of the SSD distribution in this study. The latency at which a significant difference emerged between SS and LMGO trials was estimated by looking at the first time point for which the difference exceeded the mean difference + 2 s.d. during a baseline period (a 500 ms time interval that preceded cue onset), with the additional constraint that the effect duration had to exceed 50 ms. US units preferentially responded during US trials. US units had to display a higher firing rate in a 1000-ms window after incorrect button presses than the firing rate observed during the 50% faster proportion of GO trials (aligned on button press).

Motor units (GO) responded preferentially during a 1000-ms window centered on button presses and this increase had to be superior to the firing rate observed during SS trials (we used a 1000-ms window following the stop cue to quantify stopping activity). The latency at which a significant difference emerged between US and fast GO trials (for error-related units) or between GO and SS trials (for motor-related units) was estimated using identical criteria used for SS-LMGO contrast (for inhibition-related units). Nonresponsive units corresponded to all the units that did not fulfill criteria used to define SS, US and GO units.

To determine how STN neurons mediated the three different functional responses across patients, we computed the grand-average activity separately for each group of cells, that is, units that responded significantly to inhibition (SS trials), error processing (US trials) or motor responses (GO trials). Baseline firing rate was used to compute z-scored SDFs for each cell before ensemble-averaging. We quantified the maximal spike activity using these normalized SDF during a 1000-ms time interval.

LFPs were recorded bilaterally using Medtronic 3389 DBS electrodes between 2–4 days after DBS surgery (Medtronic, Minneapolis, MN, USA). A bipolar montage was used between adjacent electrode contacts. Each



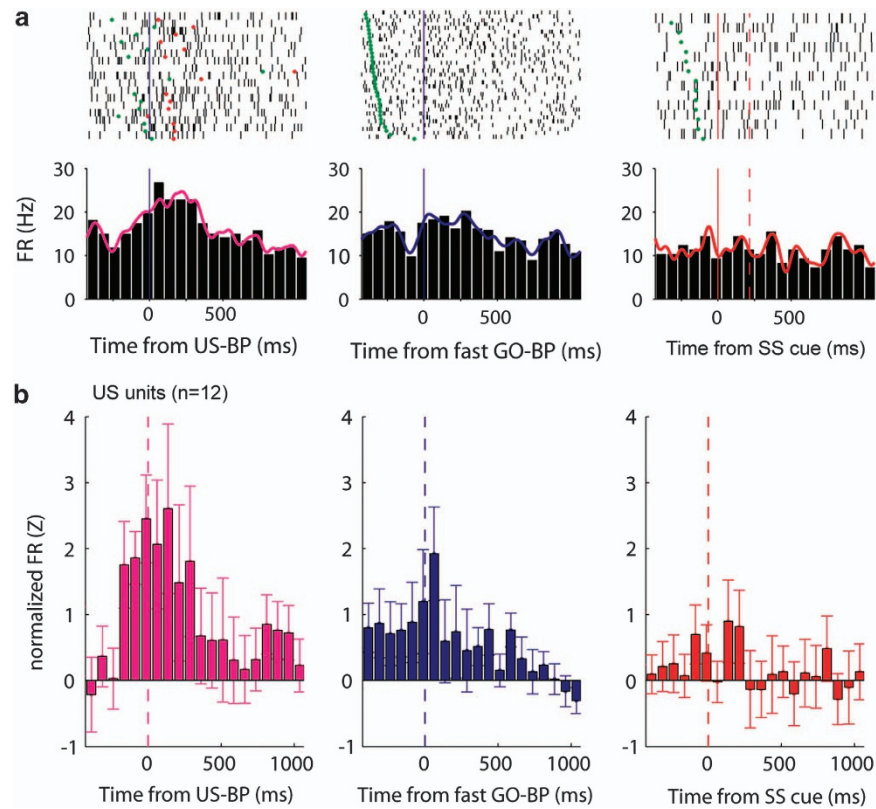


**Figure 3.** Selective response of STN neurons during error monitoring, shown as rastergrams (black dots), SDF (continuous lines) and PSTH across trial types (US, fast GO trials and SS). **(a)** Representative US unit. In rastergrams, green dots indicate the onset of GO cue and red dots indicate time of stop cue. Time origin indicates button presses (BP) during US and fast GO trials and stop cue during SS trials. **(b)** Population activity of all recorded US units ( $n = 12$ ). The conventions are as in Figure 5. PSTH, peri-stimulus spike histogram; SDF, spike density function; SS, successful stop trial; STN, subthalamic nucleus; US, unsuccessful stop trial.

bipolar signal was processed using a Morlet wavelet transform to extract instantaneous power between 1 and 150 Hz. The number of cycles of the mother wavelet was set to 7, so that the support of the kernel was 350 ms at 20 Hz. Time-frequency power was log-transformed to improve Gaussianity of the data using the fixation period (average duration 1000 ms) as a baseline. The broad-spectrum of Morlet wavelet transform analyses was used for an extensive visual inspection of responses. However, we concentrated our quantitative analyses on the 15–30 Hz activity (beta band activity, BBA). To that end, continuous bipolar LFP signals were band-pass filtered in three successive 5 Hz wide frequency bands (15–20 Hz, 20–25 Hz, 25–30 Hz) using a zero phase shift noncausal finite impulse filter with 0.5 Hz roll-off. For each frequency band, we computed the envelope of the band-pass filtered signal using a Hilbert transform, which was then normalized by its average value over the entire recording session. The instantaneous envelope was thus expressed in percentage (%) of the mean before being averaged between the three beta subbands to provide a single time series of BBA across the entire session. Based on the hypothesis that STN 15–30 Hz activity may mediate inhibitory control,<sup>17,35,36</sup> we selected the contact pair that displayed the maximum BBA across SS, US and GO trials for each hemisphere, resulting in 14 selected STN bipolar contact pairs (two per patient). The latency at which a significant difference emerged between SS and LMGO trials was estimated as the latency at which STN activity started to differ between SS and LMGO trials. A backward search from the peak of the beta band response observed during SS trials was used to avoid spurious or transient differences that may bias the detection of the latency onset. A threshold was set using the average  $\pm 2$  s.d. BBA quantified during a ( $-500$ :  $-250$  ms) baseline epoch preceding stop cues.

DBS electrode coordinates where the maximal level of BBA was recorded during the SST are given in Supplementary Table S3 and every DBS electrode is represented in patients' anatomical magnetic resonance imaging (Supplementary Figure S1).

Note that although we focused this report on the modulation BBA, higher frequencies (gamma band 50–150 Hz) and also theta (4–8 Hz) activities were also processed using the same approach. Reliable effects in the gamma band were observed in only one out of the seven patients and are not further reported. Theta activity was not modified by task conditions ( $F(2,26) = 0.643$ ;  $P = 0.53$ ; repeated measure analysis of variance performed on theta peak activity observed during a 1000-ms time window following stop cues during SS, US and LMGO trials).

## RESULTS

### Modulation of STN firing rate during executive control

In total, 32 SST experiments of 100 trials (70 GO and 30 STOP trials) were performed during the surgery by six OCD patients (patient 7 was only recorded during the postoperative study). Each subject performed two to three SST experiments per STN side, thus performing  $528 \pm 179$  SST trials (average  $\pm$  SD) when combining together left and right STN recordings. Average accuracy was  $85 \pm 11\%$  during GO trials and  $62 \pm 4\%$  during STOP trials. Reaction time was  $854 \pm 133$  ms during GO trials and the SSRT was  $242 \pm 74$  ms. As predicted by the horse-race model used to estimate the SSRT, incorrect reaction times observed during US trials were significantly shorter ( $549 \pm 153$  ms) than those observed during GO trials (paired Student's  $t$ -test,  $t(5) = 6.1$ ;  $P = 0.0017$ ). Thus, despite the stressful context of the neurosurgery procedure, OCD patients could accurately perform the SST.

After spike sorting, a total of 75 STN units were identified (52 single units and 23 multiunits). The average baseline firing rate of STN units, which was measured during 500-ms epochs of fixation, did not differ between single unit and multiunit (two-tailed

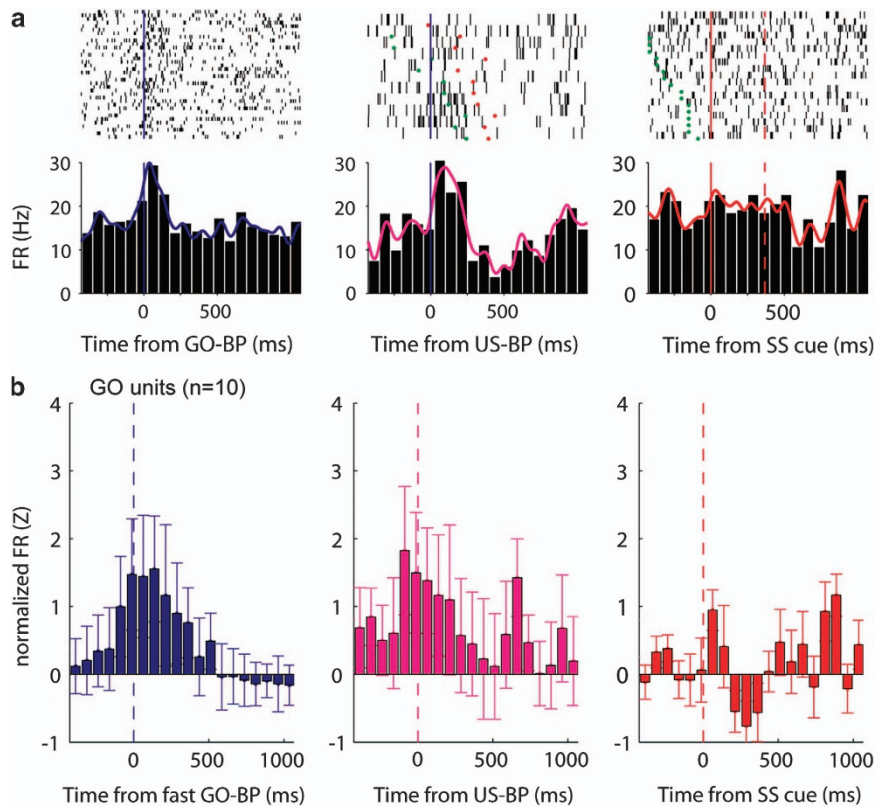


**Figure 4.** Selective response of STN neurons during motor responses, shown as rastergrams (black dots), SDF (continuous lines) and PSTH across trial types (US, GO and SS trials). **(a)** Representative GO unit. Time origin indicates button presses (BP) during US and fast GO trials and stop cue during SS trials. **(b)** Population activity of all recorded GO units ( $n=10$ ). The conventions are as in Figure 5. PSTH, peri-stimulus spike histogram; SDF, spike density function; SS, successful stop trial; STN, subthalamic nucleus; US, unsuccessful stop trial.

unpaired student's  $t$ -test,  $t(73)=0.24$ ;  $P=0.81$ ; single unit:  $19.5 \pm 11.2$  Hz; multiunit:  $20.2 \pm 13.7$  Hz) and were in accordance with STN neurophysiology known in human<sup>12</sup> and nonhuman<sup>20</sup> primates. Thirty-two of the 75 units (43%) showed a significant task-related response ( $P < 0.05$ , resampling test). We pooled the task-responsive cells into three functional classes according to their activity profile across the different conditions (GO, US, SS trials). Figure 2a shows a single cell that increased its firing rate selectively during SS trials, 167 ms before SSRT, suggesting that this neuron could in principle support a fast stopping signal. Note that this cell did not respond during US trials and GO trials. Figure 3a shows a single unit that responded after behavioral errors: it significantly increased its firing rate only during US trials ( $P < 0.05$ ) after incorrect responses, but exhibited no significant change of activity during SS trials and showed a transient decrease of activity before correct GO button presses. Figure 4a shows a third type of cell that increased its activity during motor control, that is, around correct or incorrect button presses (this increase was absent during SS trials during which there was no motor response).

To summarize group activity of cells that responded significantly to executive processes (response inhibition—SS cells—or behavioral errors—US cells) or motor events (GO cells), we computed time series and maximal value of SDFs, expressed in  $z$ -scores computed relative to a baseline level. We first supposed that STN activity should be modulated at a latency that precedes SSRT to support behavioral stopping. To test this hypothesis, the analysis of the firing rate of SS cells was restricted to a time interval defined between stop cue (or virtual stop cue) and SSRT (Figure 2b,  $n=10$ ; 13.3% of all recorded STN cells; six patients contributed to this analysis, see Supplementary Table S2). We

found that the maximal normalized firing rate of SS units was significantly higher during SS than during LMGO ( $t(9)=2.4$ ;  $P=0.038$ ) during this interval. This provides the first human single-cell evidence in agreement with the hypothesis that one of the key functions of the STN is to act as a brake to rapidly suppress inappropriate responses.

Another population of STN cells selectively responded only after behavioral errors (US cells, Figure 3b, US units,  $n=12$ , 16% of recorded units; five patients contributed to this analysis, see Supplementary Table S2). We hypothesized that US neurons could encode an error-monitoring signal. In agreement with this hypothesis, the latency at which US cells differed from the faster 50% GO trials after incorrect button presses was  $364 \pm 117$  ms.

Finally, we also found motor-related activities in the STN: GO cells (Figure 4b;  $n=10$ , 12%; six patients contributed to this analysis, see Supplementary Table S2). The latency of the firing rate increase preceded correct motor responses by  $123 \pm 84$  ms on average (GO activity was compared with SS activity to estimate this latency, see Materials and Methods).

#### Selective increase of BBA during stopping

Postoperative LFP recordings from DBS macroelectrodes in the STN were obtained two to three days after the surgery. In this second experiment, patients performed on average  $562 \pm 35$  GO trials and  $241 \pm 15$  STOP trials. During GO trials, accuracy was  $87.7 \pm 11.6\%$  and reaction time was  $711 \pm 94$  ms. From STOP trials, the SSRT was  $197 \pm 70$  ms and response accuracy during stopping was controlled to  $56.1 \pm 5.7\%$ . Reaction times were significantly shorter during US trials ( $504 \pm 83$  ms) than those observed during GO trials ( $t(6)=6.1$ ,  $P=0.0009$ ).

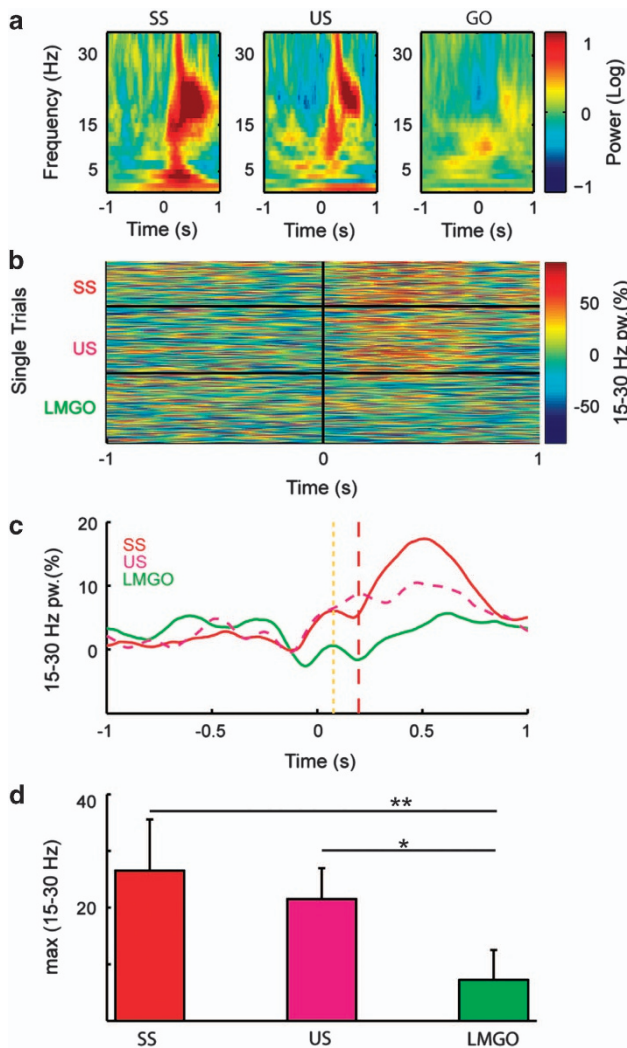


**Figure 5.** Subthalamic task-related LFP activity. **(a)** Trial-averaged time-frequency charts of a STN bipolar recording in a representative patient. Time origin indicates stop cue during SS and US trials and button press during GO trials. **(b)** Single-trial beta band power of a STN bipolar recording time-locked to stop cue during SS and US trials and to virtual stop cue during GO trials. **(c)** Grand average beta power time series ( $n = 7$  patients, 14 recorded STNs). **(d)** Beta band maximal power amplitude in the 500-ms period after stop (or virtual stop) cue. Vertical dashed orange line indicates the average latency at which the difference between SS and LMGO trials reached significance. Vertical dashed red line indicates SSRT. Stars indicate significant differences between trial types (*post hoc* Tukey,  $P < 0.05$ ). LFP, local field potential; LMGO, latency-matched GO; SS, successful stop trial; SSRT, stop-signal reaction time; STN, subthalamic nucleus; US, unsuccessful stop trial.

For each patient and each hemisphere, we analyzed task-related LFP changes of the pair of adjacent contacts that showed the largest BBA across SS, US and GO trials. LFP responses were characterized by an increase of BBA during correct stopping whereas BBA decreased around motor execution during GO trials (Figure 5a). A single-trial analysis showed that the BBA increase during SS trials was highly reproducible across stop trials (Figure 5b). Grand average ( $n = 14$  bipolar recordings) of beta activity confirmed its significant increase during SS and during US as compared with LMGO trials (50% slower GO trials—LMGO trials), in a 500 ms period following the STOP cue or virtual STOP cue (Figure 5c, analysis of variance,  $F(2,26) = 6.1$ ,  $P = 0.0068$  and Tukey *post hoc* tests  $P < 0.05$ ).

This finding is in agreement with the hypothesis that stopping would be mediated at the oscillatory level by an increase of beta activity.<sup>30</sup> To further examine the timing of this increase, we estimated the latency at which BBA significantly differentiated correct stopping from LMGO trials.<sup>30</sup> The onset latency of the differential SS-LMGO BBA significantly preceded SSRT ( $t(12) = 5.97$ ;  $P < 0.0001$ ), on average by  $123 \pm 74$  ms (note that latency could not be estimated for one out of 14 STN contact-pair because the SS-LMGO aligned on (virtual) stop cue did not exceed the mean  $\pm 2$  s.d. threshold). Because there was no significant difference between SS and US (Figure 5c), we also examined STN activity during stopping trials (average peak activity across SS and US trials) and found that it was significantly higher than during LMGO trials ( $n = 14$  contact pairs, Wilcoxon test,  $P = 0.0002$ ) during a time interval defined between stop cue and SSRT.

## DISCUSSION

Our findings provide direct electrophysiological evidence, both at the cell level and population level, for the involvement of functionally distinct STN neurons in at least two forms of executive control: action inhibition and error monitoring. Those neurons were found to be different from the motor neurons already described in the STN.<sup>37</sup>

Our results clearly demonstrate that a functional class of neurons increased their firing rate in association with successful withholding of a planned movement. Furthermore, the firing pattern of these cells was selective to successful stopping even in a time interval preceding SSRT, showing for the first time in human that these neurons are mediating executive processes underlying successful inhibitory control. This rapid increase of STN activity fits perfectly with theoretical predictions emerging from computational modeling<sup>38</sup> and significantly extends previous findings from behavioral, imaging and animal studies<sup>15,17–20,35,36</sup> by providing a simple mechanism by which inappropriate responses can be quickly canceled at the STN level. In addition, the function of this class of STN neurons was highly specialized as their activity was not modulated during incorrect stopping or during correct motor responses. Response stopping involves additional cortical regions, such as pre-supplementary motor areas<sup>39</sup> and inferior frontal gyri,<sup>15</sup> where similar functional cells probably exist and might increase activity of STN via the hyper-direct pathway. Moreover, we found that the STN is also mediating error-monitoring signals because another population of STN cells fired selectively after unsuccessful button presses during stop trials, and not during correct motor responses or successful stopping. This finding echoes previous reports showing similar types of cells in the medial frontal cortex in nonhuman primates<sup>24,25</sup> and in the STN of rats.<sup>40</sup> Thus, we speculate that STN cells contributing to inhibition might receive excitatory signals from inferior frontal cortex and pre-supplementary motor areas, whereas STN cells involved in error monitoring might receive a direct excitatory input from the anterior cingulate cortex.<sup>24</sup>

Although the nonmotor role of human STN is less debated since clinical studies showed that the STN stimulation can be used to alleviate motor and nonmotor symptoms,<sup>7,8,10</sup> direct electrophysiological evidence at the cellular level showing a clear modulation of STN during nonmotor processes was still lacking in humans. Importantly, we show here for the first time that more than 70% of task-responsive recorded neurons are involved during nonmotor functions, and that such neurons are distinct from purely motor cells, as predicted by the tripartite functional model of human STN.<sup>14,41</sup> We suggest that the STN mediates multiple cognitive functions by means of intermingled neuronal populations that receive the different cortical inputs.

At a larger spatial scale, we found that the BBA could also mediate stopping, echoing previous findings from STN recordings



in Parkinson disease.<sup>26,27</sup> Here, we extend the validity of this concept to non-dopamine-depleted patients. Our LFP findings also generalize to OCD patients' previous results obtained from Parkinsonian patients, regarding the decrease of STN BBA around movement. This suggests that the decrease of BBA would be a physiological marker of motor programming and execution rather than only reflect Parkinsonian conditions. Alternatively, it could also point to a common pathological condition between OCD and Parkinsonian patients where the STN would exhibit an abnormally high synchronization level at baseline.

Although BBA task-related modulations may be associated with stopping processes, this increase of activity was less specific than the increase observed for SS units. Hence, BBA increase was also observed during incorrect stopping trials, a finding that might reflect a lower functional sensitivity of LFPs compared with extracellular recordings. Thus, BBA increase could reflect a mixture of executive control signal (for example, stopping and monitoring signals) driven by different neuronal populations.

OCDs involve inhibitory control and error-monitoring anomalies<sup>4–6</sup> that are related to dysfunctions of the associative-limbic cortico-basal-ganglia loops. Here, we improve our understanding of the pathophysiology of OCD by describing cellular mechanisms within the STN that could be related to OCD patients' difficulty to stop inappropriate behaviors. We described STOP cells that fired only during motor inhibition and before the SSRT. We propose that they would implement stopping signals in the STN, in line with the critical role attributed to this structure within the motor inhibition network.<sup>15</sup> Assuming that compulsions might reflect a deficit of motor inhibition that is cortically driven,<sup>4</sup> it is likely that the selectivity of STN STOP cells during inhibitory processes may be driven by even faster increases of activity at the cortical level, probably in the pre-supplementary motor area and the inferior frontal gyrus.<sup>20,30,39,42</sup> Further experiments will however be necessary to demonstrate the existence of cortical STOP neurons in humans. We also described in the STN 'error-detection' neurons<sup>40</sup> that fired specifically after behavioral errors. Such activities also perfectly fit into the theoretical framework of OCD under the assumption that obsessions could correspond to a 'something is wrong' signal.<sup>3</sup> We speculate that in fact those specific cellular responses to errors within the STN may be influenced by a cortical top-down control, embedded by means of the limbic cingulate cortex-basal ganglia loop encoding error-monitoring signals.<sup>24</sup>

In conclusion, we demonstrated that the STN is segregated into functionally distinct neuronal populations that respond differently to several components of executive control. Therefore we propose that the STN is a hub in the brain's executive control system that locally processes information from multiple separate cognitive functions distributed in cortico-basal ganglia networks, for further planning, selection and execution of goal-directed behavior. In the context of OCD, we speculate that stimulating the STN would disrupt the pathological activity of the STN or its sensitivity to impaired cortical inputs, and thereby help re-establish efficient executive processes.

## CONFLICT OF INTEREST

The authors declare no conflict of interest.

## REFERENCES

- Logan GD, Cowan WB, Davis KA. On the ability to inhibit simple and choice reaction time responses: a model and a method. *J Exp Psychol Hum Percept Perform* 1984; **10**: 276–291.
- Stoet G, Snyder LH. Neural correlates of executive control functions in the monkey. *Trends Cogn Sci* 2009; **13**: 228–234.
- Aouizerate B, Guehl D, Cuny E, Rougier A, Bioulac B, Tignol J *et al*. Pathophysiology of obsessive-compulsive disorder: a necessary link between phenomenology, neuropsychology, imagery and physiology. *Prog Neurobiol* 2004; **72**: 195–221.
- Chamberlain SR, Blackwell AD, Fineberg NA, Robbins TW, Sahakian BJ. The neuropsychology of obsessive compulsive disorder: the importance of failures in cognitive and behavioural inhibition as candidate endophenotypic markers. *Neurosci Biobehav Rev* 2005; **29**: 399–419.
- Chamberlain SR, Fineberg NA, Blackwell AD, Robbins TW, Sahakian BJ. Motor inhibition and cognitive flexibility in obsessive-compulsive disorder and trichotillomania. *Am J Psychiatry* 2006; **163**: 1282–1284.
- Endrass T, Klawohn J, Schuster F, Kathmann N. Overactive performance monitoring in obsessive-compulsive disorder: ERP evidence from correct and erroneous reactions. *Neuropsychologia* 2008; **46**: 1877–1887.
- Krack P, Hariz MI, Baunez C, Guridi J, Obeso JA. Deep brain stimulation: from neurology to psychiatry? *Trends Neurosci* 2010; **33**: 474–484.
- Limousin P, Pollak P, Benazzouz A, Hoffmann D, Le Bas JF, Broussolle E *et al*. Effect of parkinsonian signs and symptoms of bilateral subthalamic nucleus stimulation. *Lancet* 1995; **345**: 91–95.
- Chabardes S, Polosan M, Krack P, Bastin J, Krainik A, David O *et al*. Deep brain stimulation for obsessive-compulsive disorder: subthalamic nucleus target. *World Neurosurg* 2012; **80**: S31.e1–8.
- Mallet L, Polosan M, Jaafari N, Baup N, Welter ML, Fontaine D *et al*. Subthalamic nucleus stimulation in severe obsessive-compulsive disorder. *N Engl J Med* 2008; **359**: 2121–2134.
- Parent A, Hazrati LN. Functional anatomy of the basal ganglia. II. The place of subthalamic nucleus and external pallidum in basal ganglia circuitry. *Brain Res Brain Res Rev* 1995; **20**: 128–154.
- Pierrat B, Polosan M, Fraix V, Goetz L, David O, Fenoy A *et al*. Subthalamic neuronal firing in obsessive-compulsive disorder and Parkinson disease. *Ann Neurol* 2011; **69**: 793–802.
- Alexander GE, DeLong MR, Strick PL. Parallel organization of functionally segregated circuits linking basal ganglia and cortex. *Annu Rev Neurosci* 1986; **9**: 357–381.
- Lambert C, Zrinzo L, Nagy Z, Lutti A, Hariz M, Foltynie T *et al*. Confirmation of functional zones within the human subthalamic nucleus: patterns of connectivity and sub-parcellation using diffusion weighted imaging. *Neuroimage* 2012; **60**: 83–94.
- Aron AR, Poldrack RA. Cortical and subcortical contributions to Stop signal response inhibition: role of the subthalamic nucleus. *J Neurosci* 2006; **26**: 2424–2433.
- van Maanen L, Brown SD, Eichele T, Wagenmakers EJ, Ho T, Serences J *et al*. Neural correlates of trial-to-trial fluctuations in response caution. *J Neurosci* 2011; **31**: 17488–17495.
- Kuhn AA, Williams D, Kupsch A, Limousin P, Hariz M, Schneider GH *et al*. Event-related beta desynchronization in human subthalamic nucleus correlates with motor performance. *Brain* 2004; **127**: 735–746.
- Baunez C, Nieuoullon A, Amalric M. In a rat model of parkinsonism, lesions of the subthalamic nucleus reverse increases of reaction time but induce a dramatic premature responding deficit. *J Neurosci* 1995; **15**: 6531–6541.
- Frank MJ, Samanta J, Moustafa AA, Sherman SJ. Hold your horses: impulsivity, deep brain stimulation, and medication in parkinsonism. *Science* 2007; **318**: 1309–1312.
- Iso M, Hikosaka O. Role for subthalamic nucleus neurons in switching from automatic to controlled eye movement. *J Neurosci* 2008; **28**: 7209–7218.
- Kuhn AA, Hariz MI, Silberstein P, Tisch S, Kupsch A, Schneider GH *et al*. Activation of the subthalamic region during emotional processing in Parkinson disease. *Neurology* 2005; **65**: 707–713.
- Kuhn AA, Brucke C, Hubl J, Schneider GH, Kupsch A, Eusebio A *et al*. Motivation modulates motor-related feedback activity in the human basal ganglia. *Curr Biol* 2008; **18**: R648–R650.
- Haynes WJ, Haber SN. The organization of prefrontal-subthalamic inputs in primates provides an anatomical substrate for both functional specificity and integration: implications for Basal Ganglia models and deep brain stimulation. *J Neurosci* 2013; **33**: 4804–4814.
- Ito S, Stuphorn V, Brown JW, Schall JD. Performance monitoring by the anterior cingulate cortex during saccade countermanding. *Science* 2003; **302**: 120–122.
- Stuphorn V, Taylor TL, Schall JD. Performance monitoring by the supplementary eye field. *Nature* 2000; **408**: 857–860.
- Alegre M, Lopez-Azcarate J, Obeso I, Wilkinson L, Rodriguez-Oroz MC, Valencia M *et al*. The subthalamic nucleus is involved in successful inhibition in the stop-signal task: a local field potential study in Parkinson's disease. *Exp Neurol* 2013; **239**: 1–12.
- Ray NJ, Brittain JS, Holland P, Joundi RA, Stein JF, Aziz TZ *et al*. The role of the subthalamic nucleus in response inhibition: evidence from local field potential recordings in the human subthalamic nucleus. *Neuroimage* 2011; **60**: 271–278.

- 28 Schall JD, Godlove DC. Current advances and pressing problems in studies of stopping. *Curr Opin Neurobiol* 2012; **22**: 1012–1021.
- 29 Schall JD, Stuphorn V, Brown JW. Monitoring and control of action by the frontal lobes. *Neuron* 2002; **36**: 309–322.
- 30 Swann N, Tandon N, Canolty R, Ellmore TM, McEvoy LK, Dreyer S *et al*. Intracranial EEG reveals a time- and frequency-specific role for the right inferior frontal gyrus and primary motor cortex in stopping initiated responses. *J Neurosci* 2009; **29**: 12675–12685.
- 31 Hanes DP, Patterson WF 2nd, Schall JD. Role of frontal eye fields in countermanding saccades: visual, movement, and fixation activity. *J Neurophysiol* 1998; **79**: 817–834.
- 32 Verbruggen F, Logan GD. Response inhibition in the stop-signal paradigm. *Trends Cogn Sci* 2008; **12**: 418–424.
- 33 Quiroga RQ, Nadasdy Z, Ben-Shaul Y. Unsupervised spike detection and sorting with wavelets and superparamagnetic clustering. *Neural Comput* 2004; **16**: 1661–1687.
- 34 Tankus A, Yeshurun Y, Fried I. An automatic measure for classifying clusters of suspected spikes into single cells versus multiunits. *J Neural Eng* 2009; **6**: 056001.
- 35 Ray NJ, Jenkinson N, Brittain J, Holland P, Joint C, Nandi D *et al*. The role of the subthalamic nucleus in response inhibition: evidence from deep brain stimulation for Parkinson's disease. *Neuropsychologia* 2009; **47**: 2828–2834.
- 36 Swann N, Poizner H, Houser M, Gould S, Greenhouse I, Cai W *et al*. Deep brain stimulation of the subthalamic nucleus alters the cortical profile of response inhibition in the beta frequency band: a scalp EEG study in Parkinson's disease. *J Neurosci* 2011; **31**: 5721–5729.
- 37 Mink JW. The basal ganglia: focused selection and inhibition of competing motor programs. *Prog Neurobiol* 1996; **50**: 381–425.
- 38 Boucher L, Palmeri TJ, Logan GD, Schall JD. Inhibitory control in mind and brain: an interactive race model of countermanding saccades. *Psychol Rev* 2007; **114**: 376–397.
- 39 Isoda M, Hikosaka O. Switching from automatic to controlled action by monkey medial frontal cortex. *Nat Neurosci* 2007; **10**: 240–248.
- 40 Lardeux S, Pernaud R, Paleressompoulle D, Baunez C. Beyond the reward pathway: coding reward magnitude and error in the rat subthalamic nucleus. *J Neurophysiol* 2009; **102**: 2526–2537.
- 41 Mallet L, Schupbach M, N'Diaye K, Remy P, Bardinet E, Czernecki V *et al*. Stimulation of subterritories of the subthalamic nucleus reveals its role in the integration of the emotional and motor aspects of behavior. *Proc Natl Acad Sci USA* 2007; **104**: 10661–10666.
- 42 Swann NC, Cai W, Conner CR, Pieters TA, Claffey MP, George JS *et al*. Roles for the pre-supplementary motor area and the right inferior frontal gyrus in stopping action: Electrophysiological responses and functional and structural connectivity. *Neuroimage* 2012; **59**: 2860–2870.



This work is licensed under a Creative Commons Attribution-NonCommercial-ShareAlike 3.0 Unported License. The images or other third party material in this article are included in the article's Creative Commons license, unless indicated otherwise in the credit line; if the material is not included under the Creative Commons license, users will need to obtain permission from the license holder to reproduce the material. To view a copy of this license, visit <http://creativecommons.org/licenses/by-nc-sa/3.0/>

Supplementary Information accompanies the paper on the Translational Psychiatry website (<http://www.nature.com/tp>)